



Perhydrolase-nanotube-paint sporicidal composites stabilized by intramolecular crosslinking

Cerasela Zoica Dinu^{a,*}, Indrakant V. Borkar^{b,c,1}, Shyam Sundhar Bale^{b,c}, Alan S. Campbell^a, Ravi S. Kane^{b,c}, Jonathan S. Dordick^{b,c,**}

^a Department of Chemical Engineering, College of Engineering and Mineral Resources, West Virginia University, Morgantown, WV 26506, USA

^b Department of Chemical and Biological Engineering, Rensselaer Nanotechnology Center, Rensselaer Polytechnic Institute, Troy, NY 12180, USA

^c Center for Biotechnology & Interdisciplinary Studies, Rensselaer Polytechnic Institute, Troy, NY 12180, USA

ARTICLE INFO

Article history:

Received 19 June 2011

Received in revised form 12 October 2011

Accepted 1 November 2011

Available online 10 November 2011

Keywords:

Carbon nanotubes

AcT

Crosslinking

Stability

Decontamination

ABSTRACT

We have developed a strategy to preserve the activity and operational stability of a large multi-subunit enzyme immobilized onto carbon nanotubes and incorporated into latex paint. Our strategy involved the intramolecular crosslinking of perhydrolase S54V (AcT, a homo-octamer) and the subsequent immobilization of the crosslinked AcT onto single-walled carbon nanotubes (SWNTs). We employed aldehyde dextran – a bulky polymeric aldehyde obtained by oxidation of dextran with sodium metaperiodate – as a crosslinking reagent. The activity of AcT crosslinked with aldehyde dextran and covalently attached to SWNTs (AcT-dex-SWNTs) was ~40% of that of native AcT and more than two-fold higher than that of enzyme immobilized directly, i.e., without crosslinking. This relatively high retention of AcT activity was consistent with the nearly complete retention of the enzyme's secondary structure upon attachment to the nanoscale support. Further incorporation of the AcT-dex-SWNTs conjugates into a latex-based paint led to active composites that were used to decontaminate *Bacillus* spores.

© 2011 Elsevier B.V. All rights reserved.

1. Introduction

AcT, isolated from *Mycobacterium smegmatis*, is a homo-octamer of 184 kDa with $72 \times 72 \times 60$ Å dimensions [1] that effectively catalyzes the perhydrolysis of propylene glycol diacetate (PGD) to generate peracetic acid (PAA) (Scheme 1), a potent decontaminant effective against bacteria, yeasts, fungi, and spores [2–4]. AcT has a perhydrolysis to hydrolysis ratio greater than 1 and an activity 50-fold higher than that of the best lipase tested [5,6]. This makes AcT a potentially valuable biocatalyst for decontaminating various surfaces if highly active and stable enzyme-based surface formulations could be developed. Nonetheless, identifying methods to improve enzyme activity and stability, particularly upon extended exposure

to the PAA product remains a formidable challenge. Moreover, the large size of AcT coupled to its relatively high degree of surface hydrophobicity may also limit its long-term use [1,6].

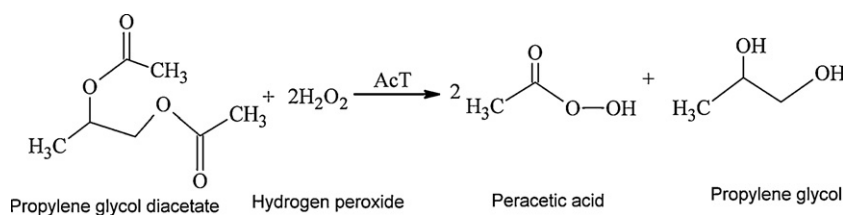
We have focused on stabilizing enzymes by attachment, both covalently and non-covalently, onto carbon nanotubes. Indeed, in the case of AcT, we have begun to test the biological decontamination of *Bacillus cereus*, a simulant of *Bacillus anthracis*, by AcT immobilized onto multi-walled carbon nanotube (MWNTs) and incorporated into polymeric films and paint composites [1]. Carbon nanotubes have excellent support characteristics due to their high surface area to volume ratios that allow relatively high enzyme loadings [7–11], ease of recovery by filtration for the enzyme-nanotube conjugate [1], and high aspect ratios that results in entrapment of the support in coatings, films and paints, thereby preventing leaching of any attached biocatalyst from the surface [1]. Critically, we hypothesize that the operational and thermal stability of a large multi-subunit enzyme such as AcT may be increased on a surface if greater rigidity of the enzyme were induced, for example, via crosslinking prior to attachment onto the nanoscale support. Along these lines, homo-bi- or poly-functional aldehydes, such as glutaraldehyde or aldehyde dextran, respectively, have been used to crosslink multimeric enzymes [12], thus increasing the rigidity of the enzyme and avoiding the formation of non-specific protein-protein associations.

* Corresponding author at: Department of Chemical Engineering, West Virginia University, College of Engineering and Mineral Resources, PO Box 6102, ESB 445, Morgantown, WV 26506, USA. Tel.: +1 304 293 9338; fax: +1 304 293 4139.

** Corresponding author at: Department of Chemical and Biological Engineering, Department of Biology, 2213 Center for Biotechnology Interdisciplinary Studies, Rensselaer Polytechnic Institute, 110 8th Street, Troy, NY 12180, USA. Tel.: +1 518 276 2899; fax: +1 518 276 2207.

E-mail addresses: cerasela-zoica.dinu@mail.wvu.edu (C.Z. Dinu), dordick@rpi.edu (J.S. Dordick).

¹ These authors contributed equally to this work.



Scheme 1.

In the current work we sought to improve AcT activity and stability when attached to single-walled carbon nanotubes (SWNTs). SWNTs were chosen as supports, as their higher surface curvature when compared with MWNTs, is expected to reduce lateral interactions between adjacent protein molecules adsorbed, leading to greater retention of native protein structure and activity. Specifically, we show that by crosslinking AcT with the polyfunctional aldehyde dextran followed by covalent attachment onto SWNTs, we can dramatically improve enzyme operational stability, thermostability, and activity of the resulting conjugates. Further incorporation of the conjugates into paint led to composites that showed complete decontamination of 10^6 Colony Forming Units (CFU)/mL of *B. cereus* spores in 60 min.

2. Results and discussion

Biological decontamination is aimed at eliminating biological hazards associated with pathogens infecting solid surfaces in laboratories [13], pilot plants [14,15], hospitals [16] or battlefield settings [17]. Decontamination involves rapid removal or neutralization of the pathogen using physical and/or chemical methods. An ideal decontaminant must be non-corrosive, non-toxic, and environmentally friendly. Enzymatic decontamination methods possess such ideal properties, since they are biodegradable, safe, easy to use, environmentally benign, and effective in low-volume doses [1,17,18]. AcT-catalyzed synthesis of PAA (Scheme 1) represents an excellent example of one such biologically driven decontamination, and thus, serves as a practical model system in this study.

Following our previous methodology [1], AcT was initially covalently attached to acid-oxidized SWNTs, which possessed carboxylic acid “handles” ideal for EDC/NHS coupling chemistry (Scheme 2a). The hydrophilic carboxyl moieties also increased nanotube dispersion and solubility [1]. Covalent attachment of AcT onto SWNTs led to enzyme loadings of 0.15 ± 0.01 mg AcT per mg SWNTs. However, AcT-SWNT conjugates retained <20% of the native solution specific activity of AcT (Fig. 1a). In contrast, when MWNTs were used as supports for AcT covalent attachment, only 8% specific activity was retained at a similar loading as that for SWNTs (see Supporting materials). This is in agreement with previous reports that show that enzyme structure and function when bound to SWNTs or silica nanoparticles are more native-like than when bound to flatter surfaces [1,19]. The hydrophobic nature of AcT (aliphatic index of 95.66, grand average hydropathicity (GRAVY) of 0.117 based on computational analysis [1]), may also lead to non-specific (and potentially unfavorable) hydrophobic interactions between the enzyme and non-functionalized hydrophobic regions of the SWNTs and MWNTs. Such interactions could be strong enough to alter enzyme structure and reduce catalytic activity. Encouraged by the higher activity retained by AcT immobilized on the SWNTs, we proceeded to use these supports in this work.

Chemical modification of proteins with crosslinkers is known to reduce non-specific interactions [12,20–22]; however, to our knowledge no work has been performed on crosslinking enzymes followed by attachment onto nanoscale supports. To that end, we

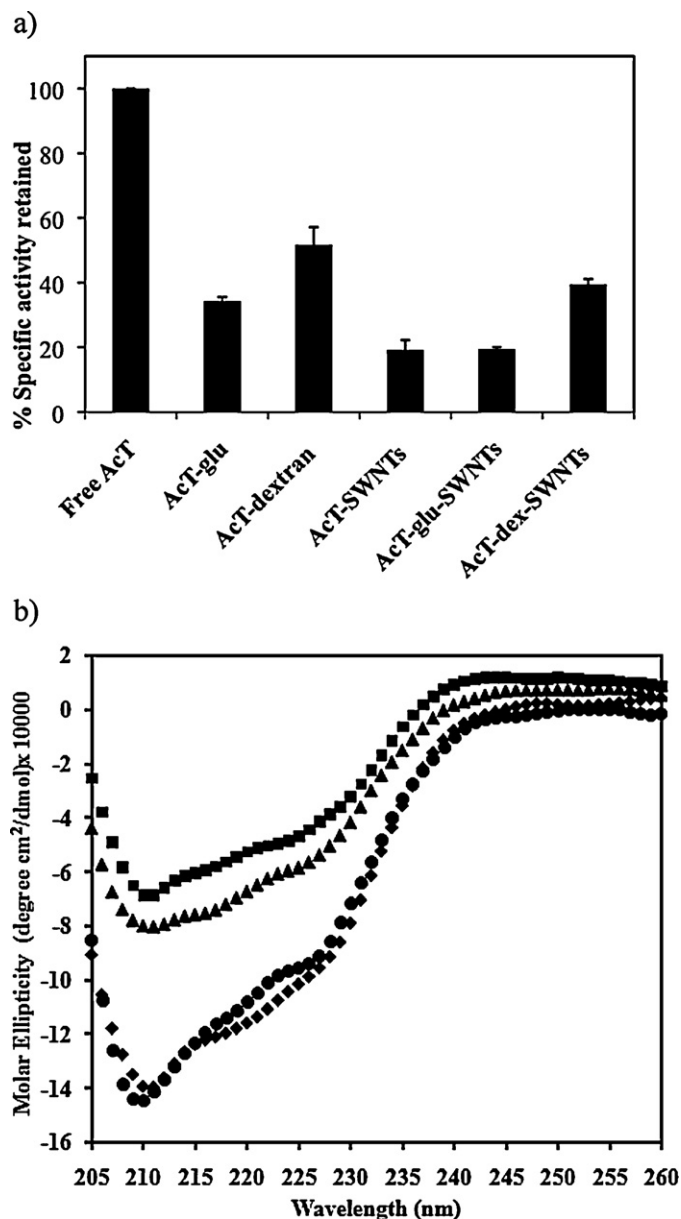
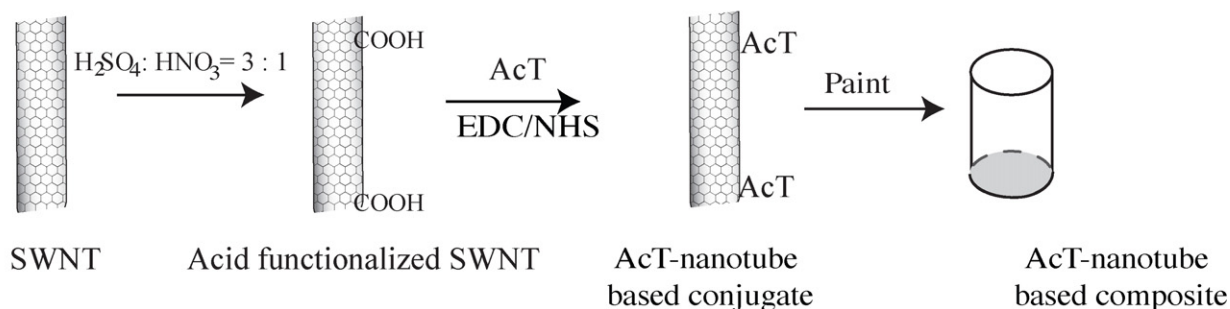


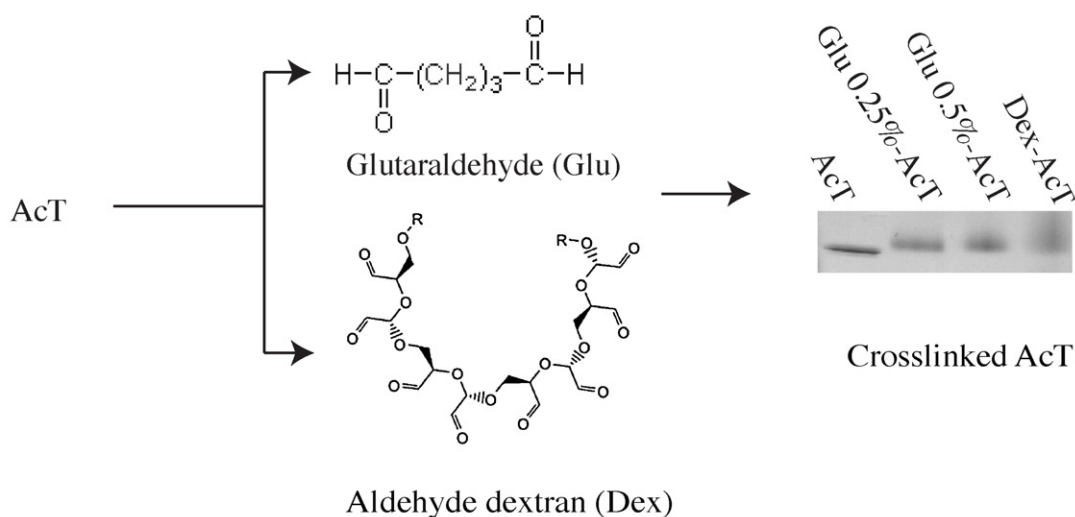
Fig. 1. (a) Specific activity of crosslinked AcT and AcT–nanotube conjugates when compared to free AcT. (b) Far-UV CD spectra of native AcT (filled diamond), AcT crosslinked with aldehyde dextran (filled circle), AcT crosslinked with 0.5% glutaraldehyde (filled square) and AcT crosslinked with 0.25% glutaraldehyde (filled triangle). At least 5 replicates were performed.

performed light crosslinking of AcT with 0.25 and 0.50% (w/w) glutaraldehyde. In both cases, the relatively light crosslinking did not result in inter-enzyme molecular linkages, as SDS-PAGE gels showed a band at roughly the same molecular weight as free AcT (Scheme 2b). No higher molecular weight bands were observed. The activity of the crosslinked AcT (AcT-glu) was ~34% of the free

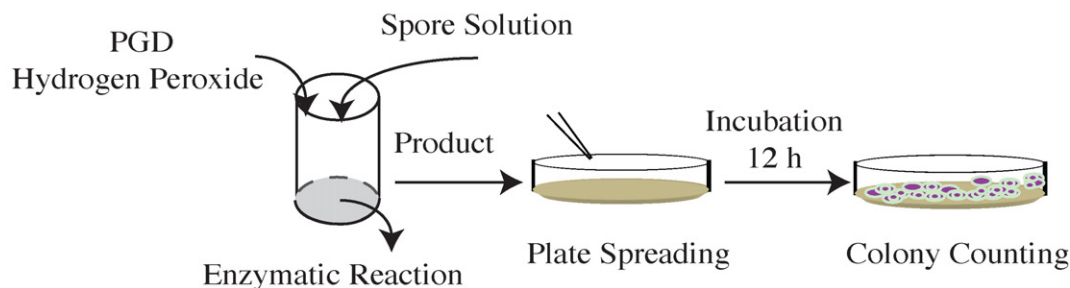
a) Preparation of AcT-based conjugates and composites



b) Preparation of crosslinked AcT



c) Decontamination of Biological Agent by Nano-based Composites



Scheme 2.

enzyme activity (Fig. 1a). We rationalized that the loss in activity may have been due to reaction of glutaraldehyde with key amino acid residues near the active site of the enzyme and/or because the small size of glutaraldehyde blocks the active site channel of AcT [12,22]. To overcome either of these deleterious outcomes, we performed light crosslinking with the polymeric aldehyde dextran prepared by oxidizing dextran (20 kDa) with sodium periodate. As with glutaraldehyde, light crosslinking with 0.25 and 0.50% (w/w) dextran aldehyde resulted in exclusively intramolecular AcT crosslinks (Scheme 2b). The somewhat diffuse band with increased

molecular weight was due to the polydispersity of the dextran aldehyde. In no case did we observe molecular weights of $2\times$ or $3\times$ of native AcT, indicating that only intramolecular crosslinking had occurred. The activity of the crosslinked AcT-dex was $\sim 52\%$ of that of free AcT (Fig. 1a). The relatively high retention of catalytic activity of the AcT-dex would suggest that the enzyme's secondary structure remained intact. Indeed, comparison of the circular dichroism (CD) spectrum of AcT-dex to that of native AcT (Fig. 1b) revealed that the enzyme retained the majority of its secondary structure, specifically $\sim 93\%$ of the native AcT α -helix content. AcT-glu, however, was

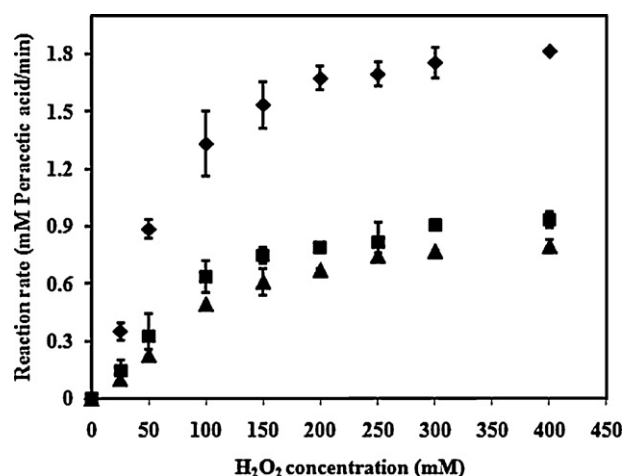


Fig. 2. Kinetics of parameters of free AcT (filled diamond), AcT crosslinked with aldehyde dextran (filled squares), and AcT crosslinked with aldehyde dextran and immobilized onto SWNTs (filled triangle). The concentration of hydrogen peroxide was varied from 0.1 mM to 428 mM while the concentration of PGD was kept constant at 200 mM. At least 5 replicates were performed.

Table 1

Kinetic parameters of free, crosslinked and immobilized AcT.

	V_m^a (mM/min)	K_m (mM)	V_m/K_m (min ⁻¹)
Free AcT	2.08	55	0.038
AcT-Dex	1.12	88	0.0125
AcT-Dex-SWNTs	1.02	110	0.0095

^a The values represent an average of measurements with standard error <7%.

structurally perturbed (Fig. 1b) with only 67% secondary structure retention even at 0.25% glutaraldehyde. This result is consistent with greater loss of activity of AcT-glu vs. AcT-dex.

To assess whether the pre-immobilization crosslinking-induced AcT stabilization by aldehyde dextran could carry over to AcT-based conjugates, we used EDC/NHS coupling to attach both glutaraldehyde- (as a comparison) and aldehyde dextran-crosslinked AcT to SWNTs in a methodology similar to that shown in Scheme 2a. AcT-glu-SWNT conjugates retained ~19% of native AcT activity, while AcT-dex-SWNT conjugates retained ~40% of native AcT activity (Fig. 1a) and nearly 80% of the activity of the AcT-dex pre-immobilized crosslinked enzyme form. In another strategy, attachment of crosslinked AcT to SWNTs was performed using an amphiphilic poly(ethylene glycol) (PEG) linker [1]. Theoretically, this type of linker could improve enzyme activity by reducing non-specific binding between the enzyme and the nanosupport, as well as it can provide more favorable orientation of the protein at the nanoscale surface [1,17]. However, no improvement in enzyme activity was observed for AcT attached to the SWNTs via the PEG linker (see Supporting material). Thus, crosslinking with the polymeric aldehyde dextran stabilizes AcT against nanotube facilitated protein deactivation.

The kinetics of AcT-dex and AcT-dex-SWNT (2 μg free or equivalent of immobilized enzyme) was studied by measuring the initial reaction rates at different substrate concentrations. The concentration of hydrogen peroxide was varied from 0.1 mM to 428 mM while the concentration of PGD was kept constant at 200 mM. AcT-dex and AcT-dex-SWNT both followed Michaelis–Menten kinetics as a function of H₂O₂ concentration (Fig. 2) with fairly similar (V_{max}/K_m) values (Table 1) and ca. 25–33% of that of the native enzyme, as a result of roughly equal contributions of lower V_{max} and higher K_m . Importantly, the relatively minor changes in both V_{max} and K_m indicate that the enzyme retained its intrinsic function following both crosslinking with aldehyde dextran and attachment to SWNTs.

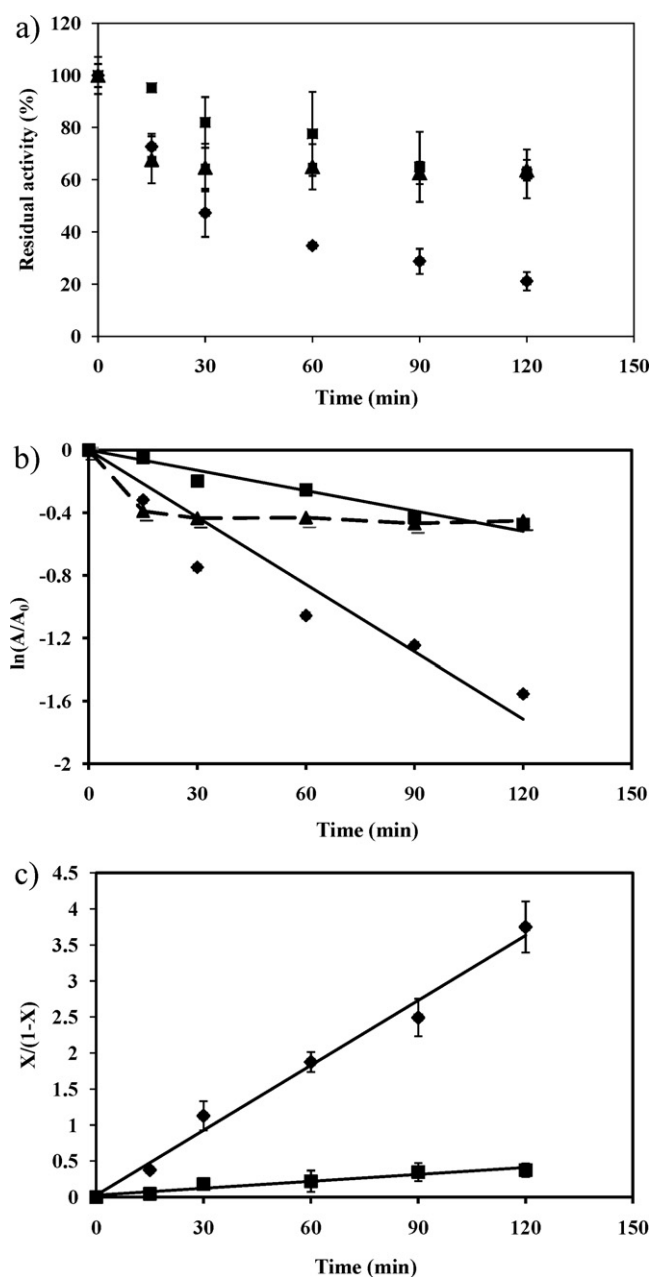


Fig. 3. (a) Thermal stability of free AcT (filled diamond), AcT crosslinked with aldehyde dextran (filled squares) and AcT crosslinked with aldehyde dextran and immobilized onto SWNTs (filled triangles) at 75 °C. (b) and (c) Deactivation plots following second order deactivation model. To confirm the data, at least 5 replicates were performed.

The combination of retained secondary structure and high activity as a result of AcT-dex crosslinking indicates that the polymeric aldehyde is restricted from gaining access to the active site and is likely causing rigidification of the multi-subunit enzyme thus leading to maintaining activity on the heterogeneous SWNT. Such rigidification would be expected to stabilize the enzyme under harsh conditions, for example, high temperature. To test this stabilization, we incubated AcT, AcT-dex, and AcT-dex-SWNTs at 75 °C for up to 2 h. While the free enzyme lost nearly 80% of its activity at 75 °C after 2 h, AcT-dex and AcT-dex-SWNTs retained more than 65% activity under these conditions (Fig. 3a). Moreover, free AcT and AcT-dex followed second order thermal deactivation (Fig. 3b and c). A typical second order thermal deactivation model is reflected

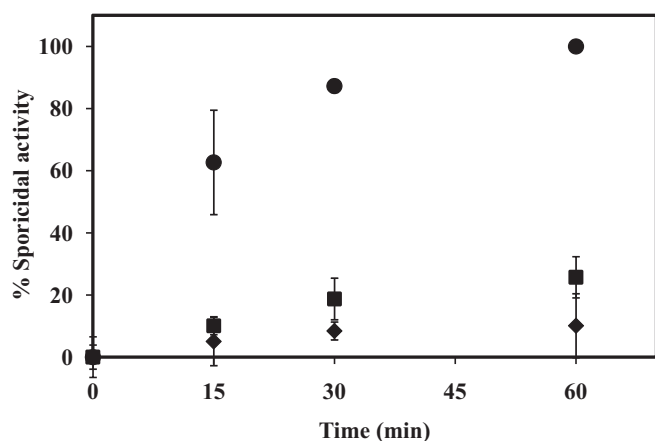


Fig. 4. Sporicidal activity of cross-linked AcT-nanotube based composites: control films (spores in buffer, filled diamond), films containing cross-linked AcT-nanotube (filled circles) and control spores in PGD and H₂O₂ reaction mixture (filled squares). At least 5 replicates were performed.

in Eq. (1), where A is the residual AcT activity and k_d is the second order deactivation rate constant.

$$\frac{dA}{dt} = -k_d A^2 \quad (1)$$

Integration of Eq. (1) within limits leads to Eq. (2) where A_0 is the initial activity of AcT and X is the fraction of enzyme deactivated.

$$\frac{X}{(1-X)} = A_0 k_d t \quad (2)$$

Plotting $X/(1-X)$ versus time confirmed second-order deactivation kinetics (Fig. 3c) and allowed determination of $A_0 k_d$ values. Half-life times ($t_{1/2}$) at 75 °C were calculated using Eq. (3), which gave values of 33 and 313 min for free AcT and AcT-dex, respectively.

$$t_{1/2} = \frac{1}{A_0 k_d} \quad (3)$$

These results are consistent with the primary deactivation of native AcT at elevated temperature being due to aggregation. AcT-dex-SWNTs do not appear to follow second order thermal deactivation (Fig. 3b), consistent with a restricted rotational degree of freedom resulting from its multi-point attachment to the nanoscale support. Further stabilization from aggregation may be due to decreased protein–protein interactions on the highly curved surface of the SWNTs [23]. In addition to thermal stability, we also studied the operational stability of AcT-dex-SWNT incubated at 4 °C for up to 180 days. No loss of activity was observed under these typical storage conditions, further confirming the high stability afforded by crosslinking of the enzyme with aldehyde dextran and attachment to the SWNT.

Motivated by the increased stability of the crosslinked enzyme bound to SWNTs, we proceeded to incorporate the crosslinked-conjugates into a latex paint (Scheme 2c) to form nanocomposites that can decontaminate *B. cereus* spores [24–29]. The high aspect ratio of the SWNTs allowed retention of the enzyme within the composite with no enzyme leaching being observed after 15 days incubation in buffer [17]. As a control, when free AcT or AcT-dex was directly added to the latex solution and dried (i.e., no nanotubes), nearly 50% of the enzyme leached out from that paint within the first 30 min. When challenged with 10⁶ CFU/mL, AcT-dex-SWNT paints (containing 0.04%, w/w, AcT) incubated in a solution containing 100 mM each of PGD and H₂O₂ generated ca. 10 mM PAA and killed >99% of the spores within 1 h (Fig. 4). Specifically, in only 15 min we achieved approximately 60% spore killing, which is in agreement with previous literature reports for direct PAA addition

[30–32]. Moreover, when the composites were challenged with 10⁶ CFU/mL of a simple non-spore forming bacterium, *E. coli*, the killing time was reduced to 5 min.

3. Conclusions

We have shown that the use of aldehyde dextran as a crosslinking agent stabilizes the native structure of AcT. The enzyme retains high activity (>40% of native aqueous solution activity) and can be incorporated into paint-based composites that have decontamination properties against *B. cereus* (a simulant of *B. anthracis*) and *E. coli*. Further work is underway to assess composite stability and activity in a wide variety of conditions (i.e., temperature, humidity, various paint compositions and polymers, etc.). The capability of generating sufficiently high concentrations of PAA makes these composites particularly useful as surface coatings for the disinfection of a wide range of pathogenic agents including bacteria and spores.

4. Experimental

4.1. AcT crosslinking with glutaraldehyde

Perhydrolase S54 (AcT, 1 mg/mL, gift from Genencor International, Inc. Palo Alto, CA, USA) was incubated at 4 °C with 0.25 and 0.50% of glutaraldehyde (Sigma, USA), respectively, for 24 h. Thus crosslinked AcT was treated with 10% (v/v) Tris–HCl buffer (1 M, pH 8, Sigma, USA). Excess reactants were removed by extensive dialysis against water at 4 °C for 24 h [33,34].

4.2. AcT crosslinking with aldehyde dextran

Aldehyde dextran was obtained by fully oxidizing 50 mL of dextran (20 kDa, 33.3 mg/mL, Sigma, USA) with sodium periodate (4.36 g, Sigma, USA) in distilled water (21, 37). After 2 h incubation in dark, the oxidized dextran was extensively dialyzed against distilled water at 4 °C for 24 h. The purified aldehyde dextran was then lyophilized for long-term storage. AcT (5 mL) in 50 mM sodium phosphate buffer (100 mM, pH 7) was added to 150 mg of aldehyde dextran (final AcT concentration was 1 mg/mL) in the presence of 150 mM trimethylaminoborane (Sigma, USA) for 24 h at 25 °C. Schiff bases, formed between the primary amino groups of the enzyme and the aldehyde groups of the polymer were reduced by the addition of 3 mg/mL sodium borohydride (Sigma, USA) at pH 10 [12]. After 30 min, the pH was decreased to 7 by the addition of HCl. Aldehyde dextran was further treated with 10% Tris–HCl (1 M, pH 8) in order to avoid non-specific crosslinking.

4.3. Crosslinking of the AcT confirmed by gel electrophoresis

Gel electrophoresis was used to confirm enzyme crosslinking. Specifically, NuPAGE® Novex® Tris–Acetate Gels (Native-PAGE) (Invitrogen, USA) of 4–12% gradient, 10-well was loaded with 25 µl sample of 0.01 mg/ml AcT or equivalent of AcT-derivates (i.e., AcT-dex, AcT-glu, etc.) prepared in Novex® Tris–Glycine Native Sample Buffer (Invitrogen, USA). Appropriate unstained molecular weight marker NativeMark™ (Invitrogen, USA) was also used. The gel run at 80 V for 120 min in Novex® Tris–Glycine Native Running Buffer and was stained with polyacrylamide pre-cast gel SimplyBlue™ Coomassie protein stain (Invitrogen, USA), 1× pre-mixed solution.

4.4. Acid oxidation of carbon nanotubes

SWNTs were purchased from Unidym, Inc. (USA) and oxidized as previously described (1). Briefly, 100 mg SWNTs were suspended

in 60 mL of 3:1 (v/v) sulfuric acid to nitric acid (H_2SO_4 : HNO_3) mixture (Fisher Scientific, USA) and sonicated at room temperature for 6 h. The acid oxidized SWNT suspension was diluted in distilled water and the mixture was filtered through 0.2 μm polycarbonate filter membrane (Millipore, USA). The SWNT “cake” that formed on the filter was resuspended in distilled water by sonication and the filtration step was repeated until water-soluble SWNTs were obtained and any insoluble impurities were removed. The SWNTs were dried under vacuum and stored at room temperature.

4.5. Functionalization of acid oxidized SWNTs with AcT and crosslinked AcT

Free and crosslinked AcT was covalently attached to 6 h oxidized SWNTs using 1-ethyl-3-[3-dimethylaminopropyl] carbodiimide hydrochloride (EDC; Acros Organics, USA) and N-hydroxysuccinimide (NHS, Pierce, USA), respectively (1). Briefly, 2 mg (SWNTs, 6 h oxidized nanotubes) were dispersed in 160 mM EDC and 80 mM NHS (total volume of 2 mL in MES (2-(N-morpholino)ethanesulfonic acid sodium salt, 50 mM, pH 4.7, Sigma) for 15 min at room temperature and 200 rpm. The activated SWNTs were next filtered through the 0.2 μm filter, washed thoroughly with MES buffer to remove any ester residues, and immediately dispersed in 1 mg/mL AcT (free, crosslinked with glutaraldehyde, or crosslinked with aldehyde dextran respectively) solution in phosphate buffer (50 mM, pH 7.0) and incubated for 3 h at room temperature with shaking at 200 rpm. The resulting AcT-based-SWNT conjugates were filtered and washed extensively with buffer to remove any unbound enzymes (1) while the supernatants and washes were collected to quantify enzyme loading.

4.6. Enzyme loading

The amount of AcT attached to SWNTs (i.e., AcT loading) was determined using standard BCA assay (bicinchoninic acid, Pierce, USA) and subtracting the amount of enzyme washed out in the filtrates from the amount of AcT initially added to the SWNTs. Briefly, the working reagent was prepared by mixing 50 parts of reagent A (BCA Protein Assay Reagent A Formulation: Bicinchoninic acid and tartrate in an alkaline carbonate buffer, <http://www.piercenet.com/browse.cfm?fldID=02020101>) with 1 part of reagent B (BCA Protein Assay Reagent B Formulation: 4% copper sulfate pentahydrate solution, <http://www.piercenet.com/browse.cfm?fldID=02020101>); subsequently 200 μl of the working reagent was incubated with 25 μl AcT-based solution. The resulting solution was incubated in 96-well plate with a clear flat bottom (Thermo Scientific, USA) at 37 °C for 30 min. Absorbance at 562 nm was determined on a Microplate reader (SpectraMax M5, Molecular Devices, Sunnyvale, CA, USA). Control calibration curves were prepared using serial dilutions of AcT (free in solution) into the working reagent.

4.7. Activity assay

AcT activity was determined by measuring the peracetic acid (PAA) generated by the free or immobilized enzyme (1). In a typical reaction, 10.6 μl hydrogen peroxide (H_2O_2 , 30%, v/v, from Sigma, USA) stock solution was added to a mixture of 0.8 mL propylene glycol diacetate (PGD, final concentration 100 mM in potassium phosphate buffer, 50 mM, pH 7.1, Sigma, USA) and 0.2 mL AcT solution (2 $\mu\text{g}/\text{ml}$ final concentration for free AcT or equivalent concentration for AcT for AcT-based conjugates). The mixture was shaken at room temperature and 200 rpm for 20 min. The PAA assay was conducted by diluting 25 μl of reaction solution 100-fold in deionized water and subsequently mixing 25 μl of the diluted solution with 75 μl deionized water and 0.9 mL assay reagent (the assay

reagent was prepared by mixing 5 mL potassium citrate buffer, 125 mM, pH 5.0 with 50 μl ABTS water solution, 100 mM, and 10 μl KI water solution, 25 mM; all the reagents were purchased from Sigma, USA). The mixture was then incubated at room temperature for 3 min and the absorbance at 420 nm was measured on a UV-vis spectrophotometer. PAA concentration was calculated as $[\text{PAA}] \text{ (mM)} = A_{420\text{nm}} \times 0.242 \times 400$ (400 is the dilution factor). The specific activity of AcT-based conjugates was calculated as the ratio of the normalized activity of the conjugates to that of the native AcT.

4.8. Circular dichroism of AcT, crosslinked AcT and AcT-based conjugates

Circular dichroism (CD) analysis was performed using a Jasco 815 Circular dichroism Spectrometer (Jasco Analytical Instruments, Inc., Easton, MD, USA). Free AcT, crosslinked AcT, and AcT-based conjugate samples were diluted in phosphate buffer to a final concentration of ca. 10 $\mu\text{g}/\text{mL}$ AcT. The CD data were collected in the range of 205–260 nm and the molar ellipticity, θ , was calculated using equation (4) where molecular weight of AcT is 184 kDa, the number of amino acids is 216 (PDB-2Q0S) and the cuvette path length is 1 cm.

$$[\theta] = \frac{\theta \times (\text{Molecular weight (kDa)} / \text{No. amino acids})}{10 \times \text{path length (cm)} \times [\text{conc}](\text{mg}/\text{mL})} \quad (4)$$

Subsequently, the residual structure of the protein in each of the cases was calculated using Eq. (5) (38).

$$\% \alpha\text{-helix} = \frac{-[\theta]_{222 \text{ nm}} + 3000}{39,000} \quad (5)$$

4.9. Kinetics of AcT, crosslinked AcT and AcT-based conjugates

Kinetics of free AcT, crosslinked AcT and AcT-nanotube conjugates was studied by measuring the initial reaction rates of the samples at different substrate concentrations. Specifically, the concentration of H_2O_2 was varied from 0.1 mM to 428 mM while the PGD concentration was maintained at 200 mM.

4.10. Thermal stability of AcT, crosslinked AcT and AcT-based conjugates

Thermal stabilities of free, crosslinked AcT and AcT-based conjugates were investigated by incubating enzyme-containing solutions in a water bath at 75 °C. Samples were collected periodically, diluted, and the activity was evaluated as previously described. The activities of different enzyme compositions were compared to the free enzyme activity.

4.11. Preparation of spores

B. cereus 4342 was purchased from ATCC (USA) and cultured in nutrient broth (3 g/L beef extract, 5 g/L peptone, Difco, USA) prepared in distilled water for 48 h. The samples were next centrifuged at 3000 rpm for 3 min and sporulation was induced by resuspending the cells in Difco Sporulation Media (DSM) at 37 °C and 200 rpm for 72 h. All reagents were purchased from Sigma, unless otherwise specified. To terminate sporulation, the solution was centrifuged at 3000 rpm for 3 min and the sediment was resuspended in distilled water; the procedure was repeated 5 times. Spore purity was determined by DIC confocal microscopy at 100 \times magnification (Nikon, NY). The spores were visibly free of germinating cells and spore concentration was estimated using standard plate count technique.

4.12. Sporidial efficiency of biocatalytic composites

Enzyme-nanotube based composites were prepared as described previously [1,17]. Briefly, water-soluble crosslinked AcT-nanotube conjugates were mixed with eco-friendly paint (Freshaire Choice™, with no volatile organic compounds, from ICI paints, Strongsville, OH, USA) in a glass vial (2.5 cm diameter, VWR, USA). The mixture was air-dried for 2 days; the resulting composite had a thickness of ~450 μm as measured by surface profilometry (Dektak 8 Surface Profiler, Veeco Instruments Inc., Plainview, NY, USA). Decontamination of spores was evaluated by incubating 10⁶ CFU/mL spores with the AcT-based composite in a reaction mixture containing 100 mM PGD and 100 mM H₂O₂ in 1 mL phosphate buffer (50 mM, pH 7), after shaking for 1 h at room temperature and 200 rpm. Aliquots from this reaction mixture were withdrawn periodically, diluted in phosphate buffer, spread onto a nutrient agar, and incubated at 37 °C for 12 h. Sporidial efficiency was determined by counting colonies grown on the agar surface and by comparing corresponding colony counts with those obtained from different controls (paint and paint with reaction mixture without enzyme, respectively).

Acknowledgements

This work was supported by DTRA (HDTRA1-08-1-0022). We thank Gregg Whited and Karl Sanford (Genencor) for the gift of AcT.

Appendix A. Supplementary data

Supplementary data associated with this article can be found, in the online version, at [doi:10.1016/j.molcatb.2011.11.003](https://doi.org/10.1016/j.molcatb.2011.11.003).

References

- [1] C.Z. Dinu, G. Zhu, S.S. Bale, G. Anand, P.J. Reeder, K. Sanford, G. Whited, R.S. Kane, J.S. Dordick, *Adv. Funct. Mater.* 20 (2010) 392–398.
- [2] D.M. Portner, R.K. Hoffman, *Appl. Environ. Microbiol.* 16 (1968) 1782–1785.
- [3] M.G.C. Baldry, *J. Appl. Microbiol.* 54 (1983) 417–423.
- [4] D. Small, W. Chang, F. Toghrol, W. Bentley, *Appl. Microbiol. Biotechnol.* 76 (2007) 1093–1105.
- [5] N.S. Amin, M.G. Boston, R.R. Bott, M.A. Cervin, E.M. Concar, M.E. Gustwiller, B.E. Jones, K. Liebeton, G.S. Miracle, H. Oh, A.J. Poulouse, S.W. Ramer, J.J. Scheibel, W. Weyler, G.M. Whited, in WIPO (Ed.), WO2005056782 (A2), C12n 9/00 ed., US, 2006.
- [6] I. Mathews, M. Soltis, M. Saldajeno, G. Ganshaw, R. Sala, W. Weyler, M.A. Cervin, G. Whited, R. Bott, *Biochemistry* 46 (2007) 8969–8979.
- [7] M.J. O'Connell, *Carbon Nanotubes; Properties and Applications*, 1 ed., CRC Taylor & Francis, Boca Raton, 2006.
- [8] A.M. Popov, Y.E. Lozovik, S. Fiorito, L. Yahia, *Int. J. Nanomed.* 2 (2007) 361–372.
- [9] M. Shim, N.W.S. Kam, R.J. Chen, Y.M. Li, H.J. Dai, *Nano Lett.* 2 (2002) 285–288.
- [10] P. Asuri, S.S. Karajanagi, E. Sellitto, D.Y. Kim, R.S. Kane, J.S. Dordick, *Biotechnol. Bioeng.* 95 (2006) 804–811.
- [11] P. Asuri, S.S. Bale, R.C. Pangule, D.A. Shah, R.S. Kane, J.S. Dordick, *Langmuir* 23 (2007) 12318–12321.
- [12] M. Fuentes, R.L. Segura, O. Abian, L. Betancor, A. Hidalgo, C. Mateo, R. Fernandez-Lafuente, J.M. Guisan, *Proteomics* 4 (2004) 2602–2607.
- [13] M.F. Verce, B. Jayaraman, T.D. Ford, S.E. Fisher, A.J. Gadgil, T.M. Carlsen, *Environ. Sci. Technol.* 14 (2008) 5765–5771.
- [14] J.B.L. Harkness, A.A. Fridman, *NCASI Tech. Bull.* (1999).
- [15] A.H. Mahvi, L. Diels, *Int. J. Environ. Sci. Technol.* 1 (2004) 199–204.
- [16] L.A. Jury, J.L. Cadnum, A. Sanders-Jennings, E.C. Eckstein, S. Chang, C.J. Donskey, *Am. J. Inf. Control* 38 (2010) 234–236.
- [17] I.V. Borkar, C.Z. Dinu, S.S. Bale, R.S. Kane, J.S. Dordick, *Biotechnol. Prog.* 26 (2010) 1622–1625.
- [18] T.C. Cheng, S.P. Harvey, G.L. Chen, *Appl. Environ. Microbiol.* 62 (1996) 1634–1641.
- [19] W. Shang, J.H. Nuffer, J.S. Dordick, R.W. Siegel, *Nano Lett.* 7 (2007) 1991.
- [20] B.G. Davis, *Curr. Opin. Biotechnol.* 14 (2003) 379–386.
- [21] L. Betancor, A. Hidalgo, G. Fernandez-Lorente, C. Mateo, R. Fernandez-Lafuente, J.M. Guisan, *Biotechnol. Prog.* 19 (2003) 763–767.
- [22] G. Penzol, P.A. Armisen, R. Fernández-Lafuente, L. Rodes, J.M. Guisán, *Biotechnol. Bioeng.* 60 (1998) 518–523.
- [23] C.Z. Dinu, S.S. Bale, G. Zhu, J.S. Dordick, *Small* 5 (2009) 310–315.
- [24] P. Wang, M.V. Sergeeva, L. Lim, J.S. Dordick, *Nat. Biotechnol.* 15 (1997) 789793.
- [25] S.J. Novick, J.S. Dordick, *Chem. Mater.* 10 (1998) 955–958.
- [26] A.B. Iqbal Gill, *Biotechnol. Bioeng.* 70 (2000) 400–410.
- [27] J. Kim, T.J. Kosto, J.C. Manimala, E.B. Nauman, J.S. Dordick, *AIChE J.* 47 (2001) 240–244.
- [28] N. Vasileva, T. Godjevargova, V. Konsulov, A. Simeonova, S. Turmanova, *J. Appl. Polym. Sci.* 101 (2006) 4334–4340.
- [29] C.S. McDaniel, J. McDaniel, M.E. Wales, J.R. Wild, *Prog. Org. Coat.* 55 (2006) 182–188.
- [30] X. Tong, A. Trivedi, H. Jia, M. Zhang, P. Wang, *Biotechnol. Prog.* 24 (2008) 714–719.
- [31] S. Leaper, *J. Food Technol.* 19 (1984) 355–360.
- [32] S. Leaper, *J. Food Technol.* 19 (1984) 695–702.
- [33] A. Alasri, M. Valverde, C. Roques, G. Michel, C. Cabassud, P. Aptel, *Can. J. Microbiol.* 39 (1993) 52–60.
- [34] J.A. Gerrard, P.K. Brown, S.E. Fayle, *Food Chem.* 79 (2002) 343–349.